Food & Function

ROYAL SOCIETY OF CHEMISTRY

PAPER

View Article Online
View Journal | View Issue

Cite this: *Food Funct.*, 2021, **12**, 83

Chemical compounds with a neuroprotective effect from the seeds of *Celosia argentea* L.†

Jinggong Guo, ‡[a] Shan Shen,‡[b,c] Xiao Zhang,[d] Guoying Wang,[e] Yiqing Lu,[f] Xiping Liu,[b] Shuyun Wang,[b] Qin Li,[b] Yue Cong *[b] and Bingyang Shi *[e,g]

Oxidative stress plays a central role in the common pathophysiology of neurodegenerative diseases such as Alzheimer's disease, amyotrophic lateral sclerosis, and Parkinson's disease. Antioxidant therapy has been suggested for the prevention and treatment of neurodegenerative diseases. Compounds derived from natural sources may offer the potential for new treatment options. *Semen Celosiae* is a traditional Chinese edible herbal medicine with a long history in China and exhibits wide-reaching biological activities such as hepatoprotective, anti-tumor, anti-diarrheal, anti-diabetic, anti-oxidant, *etc*. In this study, nine saponins and two phenylacetonitrile glycosides were isolated from *Semen Celosiae* and their structures were identified using ESI-MS and NMR techniques. Among them, compounds **1** and **2** have not been previously reported. The total concentrations of the five triterpenoid saponins and the two phenylacetonitrile glycosides were 3.348 mg g^{-1} and 0.187 mg g^{-1}, respectively, suggesting that *Semen Celosiae* is a novel viable source of the two kinds of compounds. These compounds were observed to significantly attenuate *t*-BHP-induced neuronal damage by effectively enhancing cell viability and decreasing reactive oxygen species generation and cell apoptosis rate in NSC-34 cells. Furthermore, compounds **1** and **7** reduced the ratios of cleaved caspase-3: caspase-3 and cleaved caspase-7: caspase-7 and the level of cytochrome C, while they increased the levels of SOD1 and Beclin 1. These findings suggest that compounds **1–11** are potent inhibitors of neuron injury elicited by *t*-BHP, possibly *via* inhibition of oxidative stress and apoptosis, and activation of autophagy; therefore they may be valuable leads for future therapeutic development.

Received 4th August 2020,
Accepted 18th October 2020

DOI: 10.1039/d0fo02033h

rsc.li/food-function

1. Introduction

Neurodegenerative diseases, as a heterogeneous group of disorders, are characterized by slow progressive loss of neurons. The etiology of neurodegenerative diseases has not yet been fully elucidated; however, increased oxidative stress has been suggested as one of the common etiologies of various neurodegenerative diseases.[1,2] Cumulative oxidative stress may induce cellular damage, impairment of the DNA repair system and mitochondrial dysfunction. For this reason, there have been continuing efforts to search for the agents that can protect against oxidative damage and treat neurodegenerative diseases. New natural products may be effective for the prevention or treatment of neurodegenerative conditions.

Celosia argentea L., an annual herb, belongs to the Amaranthaceae family and its mature seeds, namely *Semen Celosiae*, are commonly called "Qingxiangzi" in Chinese. As a traditional Chinese edible herbal medicine, *Semen Celosiae* is included in Chinese Pharmacopeia (2020 Edition) and is frequently used for treating ulcers, liver-heat, red eye, blurred vision, dizzy spells, *etc*. Modern pharmacological studies manifested that *Semen Celosiae* exhibits hepatoprotective, anti-infection, anti-tumor, anti-diarrheal, anti-diabetic, and anti-oxidative activities.[3,4] It is worth noting that *Semen Celosiae* can be used as both food and medicine due to its high nutritive value.[5] Recently, with the increasing extensive studies on the chemical constituents of *Semen Celosiae*, multiple classes of chemical constituents have been isolated and identified in

[a]*State Key Laboratory of Cotton Biology, School of Life Sciences, Henan University, Kaifeng, China*
[b]*Institute of Pharmacy, School of Pharmacy, Henan University, Kaifeng, China. E-mail: congyue1027@163.com; Fax: +86-371-2388 0680; Tel: +86-371-23880680*
[c]*Ludong Hospital, Yantai, China*
[d]*The Key Laboratory of Natural Medicine and Immuno-Engineering, Henan University, Kaifeng, China*
[e]*Faculty of Medicine & Health Sciences, Macquarie University, Sydney, NSW, Australia. E-mail: bingyang.shi@mq.edu.au; Fax: +86-371-2388 7799; Tel: +86-371-2388 7799*
[f]*Centre for Nanoscale BioPhotonics, Macquarie University, Sydney, NSW, Australia*
[g]*International Joint Center for Biomedical Innovation, College of Life Sciences, Henan University, Kaifeng, China*

†Electronic supplementary information (ESI) available: NMR spectra, MS, IR, and UV spectra of compounds **1–11** are shown in Fig. S1–S39; calibration curves, linear range, precision, repeatability, stability, and recovery tests of seven analytes are shown in Tables S1–S6; molecular docking analyses are given in Fig. S40–S42 and Tables S7. See DOI: 10.1039/d0fo02033h

‡Equal contributors.

different investigations, including oleanane-type triterpenoid saponins, steroidal saponins, peptides, phenols, fatty acids, *etc*.

According to the report in "Ben Cao Gang Mu", a Chinese herbal and medicinal classic, *Semen Celosiae* was described to demonstrate a protective effect on the brain. Whether this property has therapeutic benefits in neurodegenerative disorders or not requires further verification. In recent years, some studies have confirmed that oleanane-type triterpenoid saponins acted as protective agents in neurodegenerative diseases.[6–8] As such, the present work aimed to extend this finding to *Semen Celosiae* by preparatively separating active compounds to determine the concentrations of these main constituents in this species as well as using *tert*-butyl hydroperoxide (*t*-BHP) to induce oxidative stress and mimic oxidative neurotoxicity *in vitro*.[9] On this basis, the present work deeply investigated the protective effect of these compounds on *t*-BHP-induced neuronal damage in NSC-34 cells and the possible underlying mechanisms. Our study may provide the scientific basis for the development and effective use of *Semen Celosiae* against neurodegenerative diseases.

2. Materials and methods

2.1. General experimental procedures

NMR spectra were recorded on a Bruker AV400 instrument (Bruker group, Fallanden, Switzerland, 400 MHz for ^{1}H and 100 MHz for ^{13}C) with tetramethylsilane (TMS) as an internal standard.[10] The measurements of IR were carried out using a Bruker Vertex 70 (Bruker Corporation, Karlsruhe, Germany). The HR-ESI-MS and ESI-MS spectra were respectively recorded on Synapt Q/TOFMS (Waters Corporation, Milford, MA, USA) and QTRAP 4000 mass spectrometer (AB Sciex, Framingham, MA, USA) equipped with an electrospray ionization (ESI) source. MCI GEL CHP20 (Mitsubishi Chemical, Tokyo, Japan) and ODS C18 (YMC, Tokyo, Japan) were used for column chromatography. Semi-preparative HPLC was carried out using the Shimadzu SPD-10A (Shimadzu Co., Japan) and a Shimpack CLC-ODS/H column (250 mm × 20 mm, 10 μm, Shimadzu Co., Japan) attached to a Shimadzu SPD-10A UV detector. HPLC analyses were carried out using a Shimadzu LC-20AT series LC system (Shimadzu Corporation, Japan) that consisted of a vacuum degasser, quaternary pump, autosampler, a UV (SPD-20A) and a DAD (SPD-M10AVP) detector. The chromatography was carried out using a Shimadzu C18 column (250 mm × 4.6 mm, 5 μm, Shimadzu Co., Japan) at a temperature of 25 °C. The water used in all experiments was purified using a Milli-Q Plus 185 water purification system (Millipore). Dulbecco's modified Eagle's medium (DMEM) and 1640 medium were purchased from Gibco (Gaithersburg, MD, USA). *t*-BHP (70 wt% aqueous solution) was bought from Sigma-Aldrich (USA) and used without further purification. VECTASHIELD mounting medium was purchased from Vector Laboratories (USA). Other routine chemicals were obtained from Sigma-Aldrich and used without further purification.

2.2. Plant material

The seeds of *C. argentea* L. were collected from Henan Province, China in September 2014. The seeds were identified by Prof. Wangjun Yuan, Henan University. A voucher specimen (2014009) was deposited at the Institute of Pharmacy, Pharmaceutical College, Henan University, China. According to Processing Norms of Chinese Herbal Medicine in Henan Province,[11] stir-fried *Semen Celosia* was prepared by placing the cleansed *Semen Celosia* into a frying container, heating with mild fire and stir-frying it until its color deepens, a crackling sound is heard, and it becomes yellowish on the cutting surface and emits a fragrant odor.

2.3. Extraction and isolation

The fried *Semen Celosiae* (9.5 kg) were finely crushed to powder and extracted with a 50% (v/v) ethanol–water mixture using a JHBE-100A homogenate extractor (Zhijing Biotechnology Co., China) three times, which was carried out for 4 min each time. The combined extract was filtered and concentrated under reduced pressure. The extract was then subjected to macroporous resin HPD100 column chromatography with a gradient mixture of EtOH–H_2O (0 : 100 → 20 : 80 → 60 : 40 → 100 : 0) to provide three fractions: A (20% EtOH elution), B (60% EtOH elution), and C (100% EtOH elution). Fr. A (31 g) was separated over a silica-gel column with CH_2Cl_2–MeOH (10 : 1 → 8 : 1) to obtain subfr. A-1 (CH_2Cl_2–MeOH 8 : 1 elution). Subfr. A-1 was then purified by semi-preparative RP-HPLC with CH_3OH–H_2O (20 : 80, flow rate: 6 mL min^{-1}) to yield compound **10** (14 mg, TR 20 min) and compound **2** (10 mg, TR 24 min). Fr. B (73 g) was then subjected to MCI GEL CHP20 column chromatography with a gradient mixture of MeOH–H_2O (15 : 85 → 40 : 60 → 50 : 50 → 60 : 40 → 100 : 0) to provide five subfractions: B-1 (15% MeOH elution), B-2 (40% MeOH elution), B-3 (50% MeOH elution), B-4 (60% MeOH elution), and B-5 (100% MeOH elution). Subfr. B-2 was further separated on an ODS silica gel column with MeOH–H_2O (30 : 70) to obtain compound **7** (27 mg). Subfr. B-3 was further separated on the ODS silica gel column with MeOH–H_2O (40 : 60) to obtain compound **3** (56 mg), compound **5** (31 mg), and compound **6** (43 mg). Subfr. B-4 was further separated on the ODS silica gel column with MeOH–H_2O (45 : 55) to yield compound **8** (39 mg) and compound **9** (37 mg). Subfr. B-5 was further separated on a silica gel column with CH_2Cl_2–MeOH (25 : 1) to obtain compound **4** (20 mg) and with CH_2Cl_2–MeOH (5 : 1) to obtain compound **1** (17 mg) and compound **11** (25 mg).

Celosin M (1). White amorphous powder; $[\alpha]_D^{24}$ −34.8 (*c* 0.02, MeOH); UV (MeOH) λ_{max} (log ε): 210 (2.02) nm; ^{1}H and ^{13}C NMR data, see Table 1; HR-ESI-MS *m*/*z* 826.4575 ($[M + NH_4]^+$, calculated for 826.4584) and 831.4112 ($[M + Na]^+$, calculated for 831.4137).

4-Hydroxyl-phenylacetonitrile4-*O*-α-L-rhamnopyranosyl-(1→6)-β-D-glucopyranoside (2). White amorphous powder; $[\alpha]_D^{24}$ −10.8 (*c* 0.02, MeOH); UV (MeOH) λ_{max} (log ε): 222 (4.25) nm, 275 (2.15) nm; IR (KBr) ν_{max} 3500–3200, 2923, 2255, 1613, 1512,

Table 1 ^{13}C-NMR (100 MHz) data and ^{1}H-NMR (400 MHz) data for compound **1** in CD_3OD

Position	δ_C	δ_H	Position	δ_C	δ_H
1	44.3	2.10(dd, J = 10.8, 2.8 Hz), 1.18(m)	22	33.3	1.23(m), 0.89(m)
2	70.6	4.24(br.d, J = 3.2 Hz)	23	208.8	9.44(s)
3	83.8	3.85(d, J = 4.0 Hz)	24	11.7	1.32(s)
4	55.0		25	17.1	1.28(s)
5	49.3	1.36(m)	26	17.8	0.81(s)
6	21.1	158(m), 0.93(m)	27	26.5	1.16(s)
7	33.8	1.67(m), 1.50(m)	28	181.8	
8	40.9		29	33.6	0.89(s)
9	49.0	1.62(m)	30	24.0	0.92(s)
10	37.0		GlcA-1	104.6	4.38(d, J = 8.0 Hz)
11	24.0	1.51(m), 1.42(m)	GlcA-2	74.1	3.40(d, J = 8.0 Hz)
12	123.4	5.24(br.s)	GlcA-3	85.9	3.50(m)
13	145.3		GlcA-4	71.5	3.56(m)
14	43.1		GlcA-5	76.1	3.89(m)
15	28.7	171(m), 1.01(m)	GlcA-6	171.1	
16	24.6	2.03(m), 1.93(m)	$-OCH_3$	53.0	3.75(s)
17	47.6		Xyl-1	105.7	4.50(d, J = 7.6 Hz)
18	42.8	2.83(dd, J = 14.0, 3.5)	Xyl-2	75.2	3.17(m)
19	47.2	1.56(m), 1.10(m)	Xyl-3	77.5	3.41(m)
20	31.6		Xyl-4	70.6	3.46(m)
21	34.9	1.19(m), 1.36(m)	Xyl-5	67.1	3.88(m), 3.20(m)

Table 2 ^{13}C-NMR (100 MHz) data and ^{1}H-NMR (400 MHz) data for compound **2** in CD_3OD

Position	δ_C	δ_H	Position	δ_C	δ_H
1	126.0		Glc-1	102.2	4.88(d, J = 7.6 Hz)
2	130.3	7.32(d, J = 8.4 Hz)	Glc-2	74.8	3.48(m)
3	118.3	7.12(d, J = 8.4 Hz)	Glc-3	77.9	3.47(m)
4	158.6		Glc-4	71.5	3.39(m)
5	118.3	7.12(d, J = 8.4 Hz)	Glc-5	76.9	3.59(m)
6	130.3	7.32(d, J = 8.4 Hz)	Glc-6	67.8	4.02(d, J = 9.6 Hz) 3.61(m)
7	22.7	3.85(s)	Rha-1	102.1	4.72(br.d, J = 1.2 Hz)
8	119.9		Rha-2	72.3	3.71(dd, J = 3.2, 9.6 Hz)
			Rha-3	72.1	3.85(m)
			Rha-4	73.9	3.38(m)
			Rha-5	69.8	3.67(s)
			Rha-6	17.9	1.21(d, J = 6.5 Hz)

1236 cm^{-1}; ^{1}H and ^{13}C NMR data, see Table 2; HR-ESI-MS m/z 440.1546 ($[M - H]^-$, calculated for 440.1562), 476.1310 ($[M + Cl]^-$, calculated for 476.1318) and 486.1600 ($[M + HCOOH - H]^-$, calculated for 486.1617).

2.4. Determination of compound concentrations in the crude and stir-fried *Semen Celosiae*

The HPLC linear gradient profile for compounds **3**, **5**, **6**, **8**, and **9** was as follows: acetonitrile (containing 0.1% acetic acid): water (containing 0.1% acetic acid) 26 : 74 v/v −35 : 65 (0–60 min) run at a flow rate of 1 mL min^{-1}. The UV detection wavelength was set to 203 nm based on the result of ultraviolet full-wavelength scan. The injection volume was 10 μL. All 5 peaks were identified by comparing their retention times with those of the isolated compounds **3**, **5**, **6**, **8**, and **9**.

The HPLC linear gradient profile for compounds **2** and **10** was as follows: acetonitrile : water 7 : 93 v/v run at a flow rate of 1 mL min^{-1}. The UV detection wavelength was set to 220 nm based on the result of ultraviolet full-wavelength scan. The injection volume used was 10 μL. The 2 peaks were identified by comparing their retention times with those of the isolated compounds **2** and **10**.

The dried *Semen Celosiae* was ground into powder and sized by passing it through a 60 mesh. 1 g of the powder was added to 10 mL of a 50% methanol–water mixture held in an Erlenmeyer flask with a stopper and then weighed. The powder was ultrasonically extracted using a KQ 3200 apparatus (Kunshan Ultrasonic Instrument Co., China) for 30 min at 25 °C, weighed to add weight loss, and mixed with the 50% methanol–water mixture. The Erlenmeyer flask was placed on the bench for 10 min to settle. The mixture was then filtered, concentrated, and set the volume to a 1 mL volumetric flask with 50% methanol–water mixture. The sample was then filtered through a 0.22 μm microporous membrane for its analysis by LC. Standard stock solutions of analytes were respectively prepared with the 50% methanol–water mixture. Calibration curves were generated by diluting the standard stock solutions to form a series of solutions at appropriate concentrations. The precision of the dilutes was evaluated with variations in the standard mixed solution. The stability and repeatability were tested using the same sample, and its accuracy was evaluated by running recovery tests.

2.5. NSC-34 cell culture and treatments

NSC-34 cell line was obtained from the American Type Culture Collection and was grown in DMEM. The media were supplemented with 10% heat-inactivated fetal bovine serum, 100 U mL^{-1} penicillin, and 100 U mL^{-1} streptomycin. The cells were maintained at 37 °C under a humidified 5% CO_2 atmosphere.

The stock solutions of compounds **1–11** were dissolved at 10 mM in water or water containing 20% DMSO and stored at −30 °C. Before the experiment, the stock solutions were diluted with DMEM and stored at 4 °C. NSC-34 cells were pretreated with compounds **1–11** and vitamin E (Ve) for 24 h before exposure to *t*-BHP in every experiment. Cells treated with 100 μM Ve were regarded as the positive control. Cells treated with 90 μM *t*-BHP alone were used as the negative control. All cell culture assays were repeated three times.

2.6. Cell viability assay

NSC-34 cells were seeded into 96-well plates (1×10^4 cells per well) and incubated in the absence or in the presence of 2, 5 and 10 μM compounds **1–11** for 24 h. The cells were then treated with 90 μM *t*-BHP. After 6 h of incubation, according to

the manufacturer's instructions, the cell viability was determined by CCK-8 assay (Abcam, USA). A microplate reader (BGM LABTECH, Germany) was used to detect the optical density (OD) values at 450 nm (detection wavelength). These results were expressed as a ratio compared with the control group (designated as 100%).

2.7. Determination of intracellular reactive oxygen species (ROS)

The intracellular ROS level was assessed using a combination of flow cytometry and cellular imaging. The generation of reactive oxygen species was detected using Cell ROX™ Deep Red Reagent (Invitrogen, USA). In brief, NSC-34 cells were seeded into 24-well plates (4×10^4 cells per well) and cultured at 37 °C for 24 h. The cells were pretreated with 2 μM compounds **1–11** for 24 h alone and then 200 μM *t*-BHP was added to them. The plate was incubated at 37 °C for 0.5 h. CellROX reagent was added to each well at a final concentration of 5 μM, and the plate was incubated for 30 minutes. The cells were washed three times with phosphate buffered saline (PBS). The cells were harvested by trypsinization and fixed in 3% formaldehyde for 10 minutes. The fixed cells were collected by centrifugation and resuspended in 0.5 mL of PBS for BD LSRFortessa X-20 flow cytometry (BD Biosciences, USA) analysis using a 647 nm laser and a 670 nm filter.

For cellular imaging, NSC-34 cells were seeded at a concentration of 4×10^4 cells per well into 24-well plates containing glass slide covers and cultured at 37 °C for 24 h by following the above-mentioned procedure. 5 μM CellROX reagent was added to each well and the cells were incubated at 37 °C for 30 min, followed by washing with PBS (×2). Subsequently, the cells were fixed with a 4% paraformaldehyde solution for 15 min followed by washing with PBS (×2) and then stained with Hoechst 33342 (Sigma, St Louis, MO, USA) for 15 min at room temperature. Then the cells were washed twice with PBS and VECTASHIELD mounting medium was added. The cells were imaged with a Zeiss LSM 880 laser-scanning confocal microscope (Zeiss, Germany).

2.8. Annexin V-FITC apoptosis detection

An Annexin V-FITC cell apoptosis detection kit (Abcam, USA) was used to detect the apoptosis rate. NSC-34 cells were seeded at a concentration of 1×10^5 cells per well into a 12-well plate and cultured at 37 °C for 24 h. Dosage and treatment with or without compounds **1–11** were the same as those used for the cell viability tests. The NSC-34 cells were collected by trypsinization and washed once with PBS (pH 7.4). Finally, the cells were resuspended in 500 μL of binding buffer and incubated with 5 μL of Annexin V-FITC and 5 μL of propidium iodide (PI) at room temperature for 5 min in the dark before detection. The cell apoptosis rate was measured by flow cytometry.

2.9. Western blot analysis

NSC-34 cells were cultured in six-well plates (2×10^5 cells per well) for 24 h, and the neurons were collected after each treatment. The collected cells were lysed in ice cold RIPA lysis buffer (Sigma-Aldrich, USA) for 15 min and then centrifuged at 15 000 rpm for 15 min at 4 °C. The protein concentration was determined using a Bio-Rad protein assay kit following the manufacturer's guide. Protein was separated on 12% SDSPAGE gel and transferred onto a nitrocellulose membrane. After blocking for 1 h, the membrane was incubated with primary antibodies (rabbit, 1 : 1000, Cell Signaling Technology, USA) at 4 °C overnight, washed three times with TBST, incubated with the secondary antibody (anti-rabbit, 1 : 5000, LI-COR, USA) for 1 h, and re-washed three times with TBST. The protein band was measured using an ODYSSEY CLx Infrared imaging system (LI-COR, USA), and the results were visualized using Image Studio Lite 5.2.

2.10. Molecular docking

The crystal structure of Mus musculus KEAP1 is retrieved from the RCSB Protein Data Bank (PDB ID: 6QMC) (http://www.rcsb.org/). Molecular docking studies were performed using Discovery Studio 2016. In the preparation of the protein, water and the co-crystallized ligand were removed and hydrogens were added. The KEAP1 protein was further disposed with the protein preparation module. The protonation state of each ionic residue was calculated and the conformation of the protein was optimized. The prepared protein was regarded as the receptor, and the binding site was defined by the PDB site record on the basis of the location of the ligand in 6QMC. The molecules were docked into the binding site by using the CDDOCK method. The output complex of protein–ligand was rendered with PyMol.

2.11. Statistical analysis

The results of all statistical analyses were presented as mean ± SD. One-way analysis of variance was used to analyze significant differences between the groups. A value of $P < 0.05$ was considered to be significant, and all graphs were generated using the Origin 2015 software.

3. Results

3.1. Elucidation of compound structures

The 50% ethanol extract of *Semen Celosiae* was successively chromatographed with a HPD100, silica gel, MCI gel, ODS and then purified by semipreparative HPLC to obtain the 11 compounds, among which compounds **1** and **2** are new. The chemical structures of these compounds are shown in Fig. 1.

Compound **1** was obtained as a white amorphous powder. Its molecular formula was $C_{42}H_{64}O_{15}$ as determined by HR-ESI-MS ions at *m*/*z* 826.4575 ($[M + NH_4]^+$, $C_{42}H_{68}O_{15}N$ calculated for 826.4584, 1.1 ppm) and 831.4112 ($[M + Na]^+$, $C_{42}H_{64}O_{15}Na$ calculated for 831.4137, 3.0 ppm). The ^1H NMR spectrum of compound **1** exhibited one aldehyde proton signal at δ 9.44 (1H, s, H-23), two anomeric proton signals at δ 4.50 (1H, d, J = 7.5 Hz, H-Xyl-1) and 4.38 (1H, d, J = 8.0 Hz, H-GlcA-1), one olefinic proton signal at δ 5.24 (1H, br.s, H-12), one methoxy proton signal at δ 3.75 (s, OCH_3) and six methyl

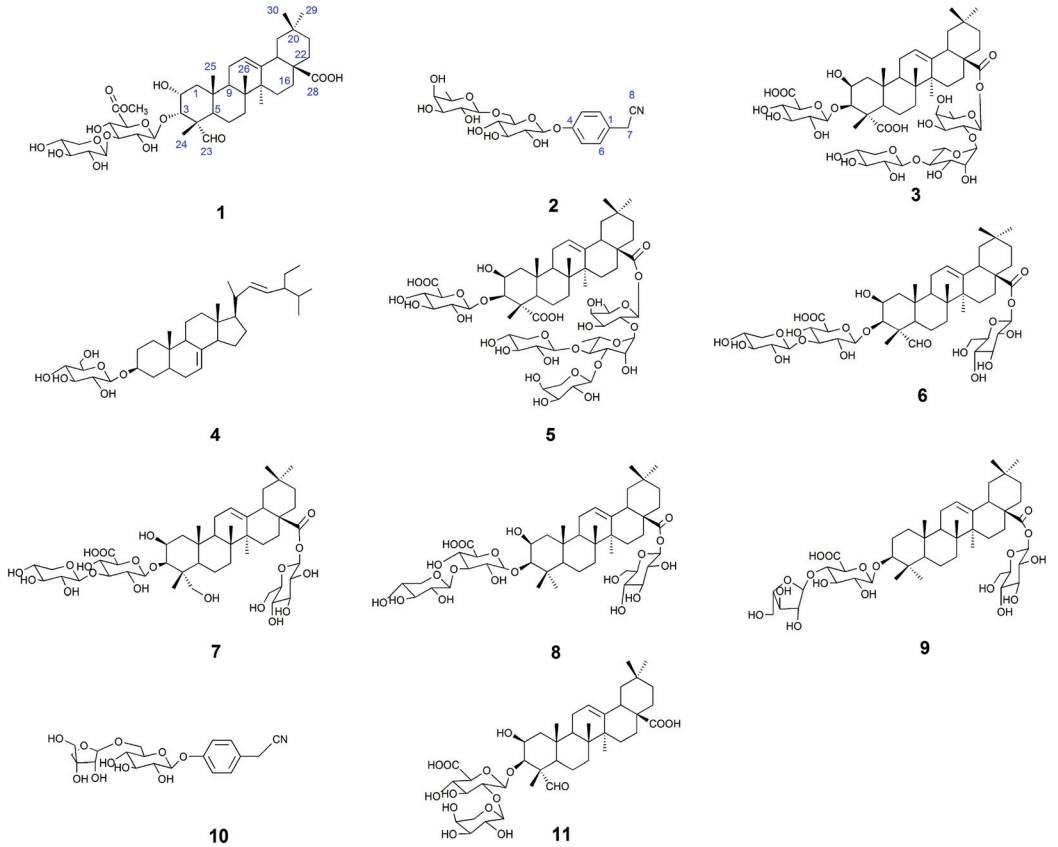

Fig. 1 Structures of compounds **1–11**.

proton signals at δ 0.81 (3H, s, CH_3-29), 0.89 (3H, s, CH_3-30), 0.93 (3H, s, CH_3-26), 1.16 (3H, s, CH_3-27), 1.28 (3H, s, CH_3-25), and 1.32 (3H, s, CH_3-24). The ^{13}C NMR spectrum contained 42 signals, which included three carbonyl carbon signals at δ 208.8 (C-23), 181.8 (C-28), and 171.1 (C-GlcA-6), two olefinic carbon signals at δ 145.3 (C-13) and 123.4 (C-12), one methoxy carbon signal at δ 53.0 and two anomeric carbon signals at δ 105.7 (C-Xyl-1) and 104.6 (C-GlcA-1), revealing that compound **1** contained two sugar units. The β-configurations of D-glucuronic acid and D-xylose were determined by the $J_{1,2}$ values of 7.8 Hz and 7.6 Hz, respectively.[12,13] A comparison of the ^{13}C NMR data of **1** with those of celosin L isolated from *Semen celosiae* showed that the structure of **1** was nearly identical to that of celosin L, except for an additional methoxy signal as well as α-orientations of the substituents at 2,3-position of compound **1**.[14,15] A combined analysis of the ^{1}H NMR, ^{13}C NMR, HSQC, and HMBC spectra showed that the methoxy signal was attached to C-GlcA-6, indicating the present of a methyl ester group, and all their proton and carbon signals were assigned (Table 1). The glycosylation positions and sugar sequence of compound **1** were confirmed by the two long-range HMBC correlations (Fig. 2) of H-1′ of GlcA at δ 4.38 with C-3 at δ 83.8, and H-1″ of Xyl at δ 4.50 with C-3′ of GlcA at δ 85.9. In the NOESY spectrum (Fig. 2), the NOE cross-peaks were observed between H–C(2) and H–C(3), Me(24), Me(25), between H–C(3) and H–C(2), Me(24), Me(25), between H–C(5) and H–C(23), between Me(25) and Me(26), and between H–C (18) and Me(27), Me(29), confirming β-positions of H–C(2), H–C(3), Me(24), Me(25), and Me(26) and α-orientations of H–C (18), H–C(23), Me(27), and Me(29). Consequently, the structure of compound **1** was elucidated as 2α-hydroxyl-23-aldehyde-3α-*O*-β-D-xylopyranosyl-(1→3)-β-D-(6′-methyl)-glucuronopyranosyl-oleanolic acid, named celosin M.

Compound **2** was obtained as a white amorphous powder. Its molecular formula was $C_{20}H_{27}O_{10}N$ as determined from HR-ESI-MS ions at *m*/*z* 440.1546 ($[M - H]^-$, $C_{20}H_{26}O_{10}N$ calculated for 440.1562, 3.6 ppm), 476.1310 ($[M + Cl]^-$, $C_{20}H_{27}O_{10}NCl$ calculated for 476.1318, 1.7 ppm) and 486.1600 ($[M + HCOOH - H]^-$, $C_{21}H_{28}O_{12}N$ calculated for 486.1617, 3.5 ppm). A sharp IR absorption band at 2255 cm^{-1} indicated the presence of a CN group[16] and this was proved by the presence of a quaternary carbon signal at δ 119.9 (C-8) in the ^{13}C NMR spectrum. The ^{1}H NMR spectrum of compound **2** exhibited two anomeric proton signals at δ 4.72 (1H, br.d, J = 1.2 Hz, H-Rha-1) and 4.88 (1H, d, J = 7.6 Hz, H-Glc-1), and four aromatic proton signals at δ 7.32 (2H, d, J = 8.4 Hz, H-2, 6), 7.12 (1H, d, J = 8.4 Hz, H-3, 5). The ^{13}C NMR spectrum contained 20 signals, which included six aromatic carbon signals at δ 126.0 (C-1), 130.3 (C-2, 6), 118.3 (C-3, 5), 158.6 (C-4) and two anomeric carbon signals at δ 102.2 (Glc-1) and 102.1 (Rha-1). In HMBC, there were two long-range HMBC correlations (Fig. 3) of H-1′ of Glc at δ 4.88 with C-4 at δ 158.6, and H-1″ of

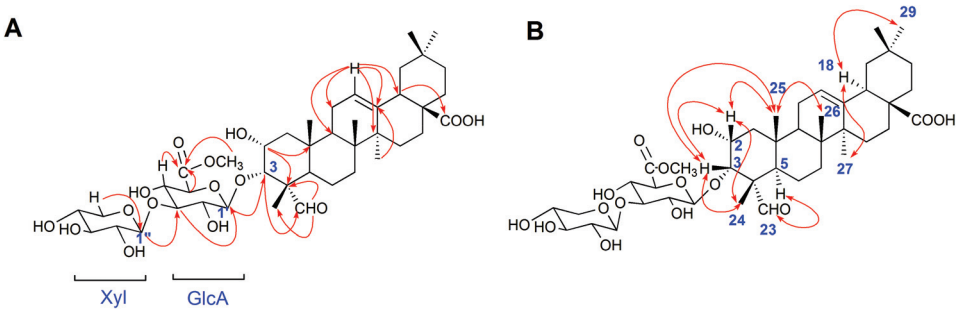

Fig. 2 (A) Key HMBC correlations and (B) key NOE correlations for compound **1**.

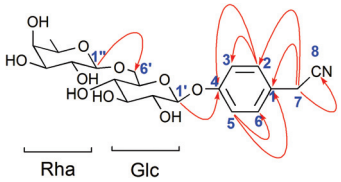

Fig. 3 Key HMBC correlations for compound **2**.

Rha at δ 4.72 with C-6′ of Glc at δ 67.8, suggesting the existence of a sugar linkage of α-L-rhamnopyranosyl-(1→6)-β-D-glucopyranosyl and the attachment of the sugar moiety at C-4 of the aromatic ring. Besides, long-range HMBC correlations were observed between H-7 (δ 3.85) and C-1 (δ 126.0), C-2 (δ 130.3), C-8 (δ 119.9), indicating that the acetonitrile group was attached at C-1 of the aromatic ring. A comparison of the ^{13}C NMR data of compound **2** with those of adenophoraside C, isolated from *Adenophora* roots,[17] showed that the structure of compound **2** was nearly identical to that of adenophoraside C, except for an additional methoxy signal of adenophoraside C. The β-configuration of D-glucose and α-configuration of L-rhamnose were determined by the $J_{1,2}$ values of 7.6 Hz and 1.2 Hz, respectively. Consequently, the structure of **2** was elucidated as 4-hydroxyl-phenylacetonitrile 4-*O*-α-L-rhamnopyranosyl-(1→6)-β-D-glucopyranoside.

Compounds **3–11** were respectively identified as celosin I (**3**),[18] α-spinasterol-3-*O*-β-D-glucopyranoside (**4**),[19] celosin J (**5**),[18] celosin H (**6**),[18] 2β, 23-dihydroxy-3-*O*-[β-D-xylopyranosyl-(1→3)-β-D-glucuronopyranosyl]-28-*O*-β-D-glucopyranosyl-oleanolic acid (**7**),[20] celosin K (**8**),[20] chikusetsusaponin IV (**9**),[21] 4-hydroxyl-phenylacetonitrile 4-*O*-β-D-apiofuranosyl-(1→6)-β-D-glucopyranoside (**10**)[16] and celosin A (**11**)[22] by various spectral analysis and comparison with the literature values. It is worth noting that compounds **4**, **7**, **9**, and **10** were obtained for the first time from the title plant.

3.2. Determination of the concentrations of compounds 3, 5, 6, 8, and 9 by HPLC-UV quantitative analysis

The proposed HPLC method for the determination of the five analytes (Fig. 4) showed good linearity (r > 0.9992) (ESI, Table S1†). The precision, stability, and repeatability were all less than 1.79%. The overall recoveries were between 97.5 and 102.8% with an RSD value of less than 2.91% (ESI, Tables S2 and S3†). The developed method was applied to determine the sample (n = 3). The average amounts of compounds **3**, **5**, **6**, **8**, and **9** are listed in Table 3. The total concentrations of the five

Table 3 The contents of the five compounds from the stir-fried and crude *Semen Celosiae* ($\bar{x}$ ± SD, n = 3)

Analytes	Stir-fried product (mg g^{-1})	Crude product (mg g^{-1})
Compound **3**	1.419 ± 0.02	1.355 ± 0.004
Compound **5**	0.831 ± 0.01	0.857 ± 0.008
Compound **6**	0.822 ± 0.005	0.862 ± 0.01
Compound **8**	0.115 ± 0.001	0.149 ± 0.0001
Compound **9**	0.161 ± 0.002	0.124 ± 0.01
Total concentration	3.348	3.247

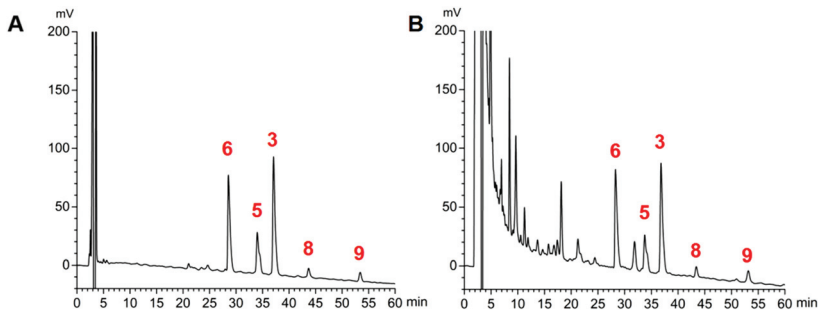

Fig. 4 HPLC chromatograms of reference substances (compounds **3**, **5**, **6**, **8**, and **9**) (A) and a sample of stir-fried *Semen Celosiae* (B).

compounds extracted from the stir-fried and crude *Semen Celosiae* were 3.348 and 3.247 mg g^{-1}, respectively.

3.3. Determination of the concentrations of compounds 2 and 10 by HPLC-UV quantitative analysis

The proposed HPLC method for the measurement of the two analytes (Fig. 5) manifested good linearity (r = 0.9999) (ESI, Table S4†). The precision, stability, and repeatability were all less than 1.30%. The overall recoveries were 99.1 and 100.6% with an RSD value of less than 2.40% (ESI, Tables S5 and S6†). The developed method was implemented to determine the sample (n = 3). The average amounts of compounds **2** and **10** are listed in Table 4. The whole content of the two compounds extracted from the stir-fried and crude *Semen Celosiae* was 0.187 and 0.171 mg g^{-1}, respectively.

3.4. Compounds 1–11 increased the cell viability and reduced *t*-BHP-induced NSC-34 cell damage

A CCK-8 assay was performed to determine whether compounds **1–11** exert any overt toxic effects on NSC-34 cells; compounds **1–11** (1–50 μM) alone for 24 h did not alter the viability of NSC-34 cells. Consequently, 2 μM, 5 μM, and 10 μM were chosen as the experimental concentrations of compounds **1–11** in anti-*t*-BHP neurotoxicity studies. After treatment with *t*-BHP ranging in concentration from 0 to 200 μM for 6 h to ensure a working dose, the neuronal cell viability was evaluated with the CCK-8 assay. *t*-BHP reduced the cell viability of NSC-34 cells in a concentration-dependent manner. Exposure to 90 μM *t*-BHP significantly decreased the cell viability to 60.6% of that of the vehicle-treated controls. Before exposure to *t*-BHP at 90 μM for 6 h, NSC-34 cells were individually pretreated with 2 μM, 5 μM, and 10 μM compounds **1–11** for 24 h. *t*-BHP-induced anti-cell proliferation was apparently attenuated by pretreatment of cells with compounds **1–11**, as shown in Fig. 6. The attenuation effects of compounds **2–6**, **8**, **9**, and **11** were found to act in a dose-dependent manner (Fig. 6).

3.5. Compounds 1–11 reduced intracellular ROS in *t*-BHP-treated NSC-34 cells

Oxidative stress evoked by abundant intracellular ROS generation is widely regarded as a possible mechanism upstream of *t*-BHP-induced cell damage. The production of ROS in *t*-BHP-treated NSC-34 cells measured by flow cytometry was increased to approximately 15 times that of the control group (Fig. 7). However, pretreatment with 2 μM compounds **1–11** significantly reduced *t*-BHP-induced ROS generation (P < 0.01; P < 0.05). Compounds **1**, **2**, **3**, **5**, **6**, **8**, and **10** exhibited a stronger ability to eliminate ROS than Ve (positive group). Similarly, the change in the intracellular ROS levels was visualized using confocal microscopy (Fig. 8). No obvious red fluorescence was observed in the cytoplasm of the control group, but strongly positive red fluorescence was detected in the cytoplasm of the *t*-BHP group. Pretreatment with compounds **1–11** significantly alleviated the proliferation of ROS induced by *t*-BHP, as observed by the reduced intensity of cell ROX fluorescence, which was in accordance with the ROS level results. Therefore, compounds **1–11** successfully decreased *t*-BHP-induced ROS generation. Among them, compounds **1** and **7** exhibited excellent attenuation of intracellular excess ROS production.

3.6. Compounds 1–11 attenuated *t*-BHP-induced apoptosis in NSC-34 cells

To investigate the protective effect of compounds **1–11** on the *t*-BHP-induced apoptosis of NSC-34 cells, the apoptosis rate of NSC-34 cells was evaluated by flow cytometry through FITC-Annexin V/PI double staining. As shown in Fig. 9, the apoptosis rate of the *t*-BHP group was obviously higher than that of the control group (P < 0.01). The apoptosis rate of cells treated with 90 μM *t*-BHP alone was 29.3%. When treated with 2 μM compounds **1–11**, the apoptosis rate decreased to the range from 15.7% to 26.2%. Moreover, all compounds except compound **6** displayed greater anti-apoptotic potential than Ve, among which compound **2** showed the best capacity on alleviation of *t*-BHP-induced apoptosis in NSC-34 cells. These results indicated that compounds **1–11** can attenuate *t*-BHP-

Table 4 The contents of the two compounds from the stir-fried and crude *Semen Celosiae* ($\bar{x} \pm$ SD, n = 3)

Analytes	Stir-fried product (mg g^{-1})	Crude product (mg g^{-1})
Compound **2**	0.097 ± 0.001	0.081 ± 0.003
Compound **10**	0.090 ± 0.001	0.090 ± 0.002
Total concentration	0.187	0.171

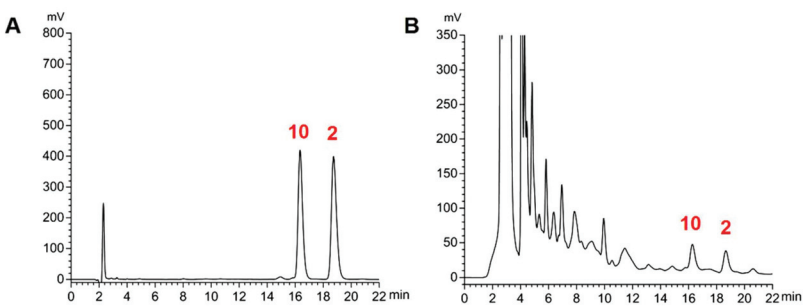

Fig. 5 HPLC chromatograms of reference substances (compounds **2** and **10**) (A) and a sample of stir-fried *Semen Celosiae* (B).

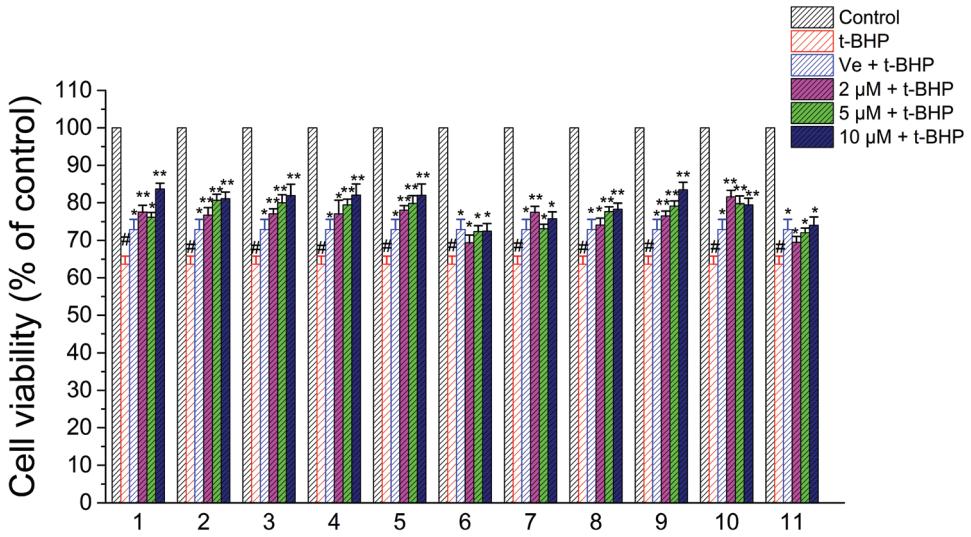

Fig. 6 Effects of compounds **1–11** on the viability of NSC-34 cells after treatment with *t*-BHP. #, $P < 0.01$ *versus* the control group; **, $P < 0.01$, *, $P < 0.05$ *versus* the *t*-BHP group.

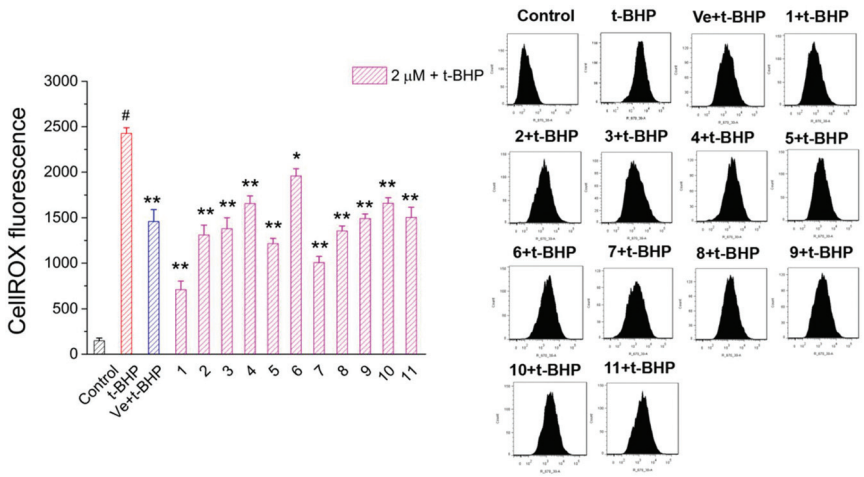

Fig. 7 ROS levels were assayed by measuring the fluorescence intensity of CellROX. #, $P < 0.01$ *versus* the control group; **, $P < 0.01$, *, $P < 0.05$ *versus* the *t*-BHP group.

induced damage and protect apoptotic cells to a certain extent at a dose of 2 μM.

3.7. Compounds 1 and 7 prevented the *t*-BHP-induced expression of apoptosis-related proteins in NSC-34 cells

To further investigate the antiapoptotic role of compounds **1** and **7** in *t*-BHP-induced neuronal damage, the levels of apoptosis-related proteins were detected in NSC-34 cells by western blotting. The expression of cleaved caspase-3, cleaved caspase-7 and cytochrome C was obviously increased in the *t*-BHP group compared with that in the control group ($P < 0.05$; Fig. 10). In contrast, pretreatment with compounds **1** and **7** can successfully reduce the expression of cleaved caspase-3, cleaved caspase-7 and cytochrome C. The ratios of cleaved caspase-3: caspase-3 and cleaved caspase-7: caspase-7 were also significantly decreased in the compound **1** + *t*-BHP and compound **7** + *t*-BHP groups compared with those in the *t*-BHP group ($P < 0.05$; Fig. 10). These results further demonstrated the roles of compounds **1** and **7** in preventing NSC-34 cells from *t*-BHP-induced neuronal injury.

3.8 Compounds 1 and 7 increased the *t*-BHP-induced expression of SOD1, Keap1 and Beclin 1 in NSC-34 cells

The expression of SOD1, Keap1, and Beclin 1 was obviously decreased in the *t*-BHP group compared with that in the control group ($P < 0.05$; Fig. 11), while interestingly, pre-treatment with compounds **1** and **7** restored the levels of Beclin-1 and SOD1 after exposure to 90 μM *t*-BHP for 6 h ($P < 0.05$; Fig. 11). Compared to the *t*-BHP group, Keap1 was upregulated in response to compounds **1** and **7**, but no significant difference was observed.

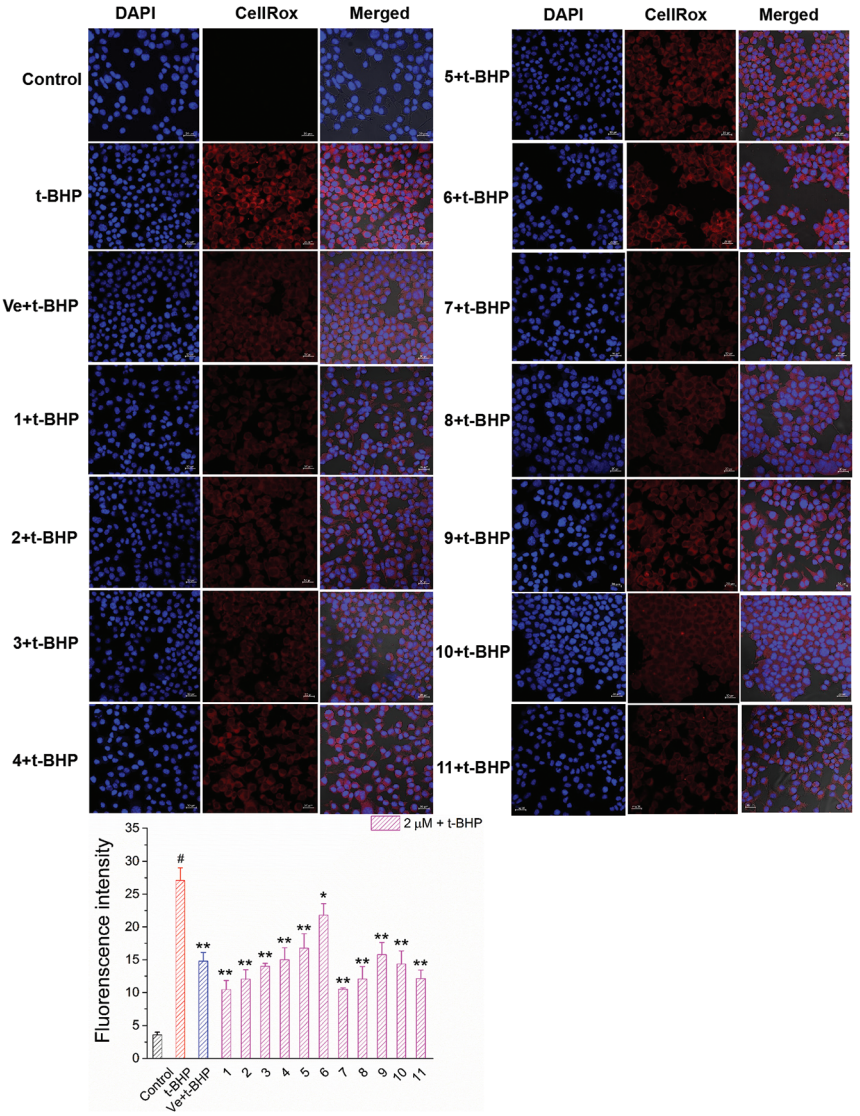

Fig. 8 Images of accumulation and elimination of ROS in NSC-34 cells. Scale bar = 20 μm. Average fluorescence intensity values were quantified using ImageJ software.

4. Discussion

The stems, leaves, and seedlings of *Celosia argentea* L. are delicious edible wild herbs with good quality. Seed sources of *Celosia argentea* L. are distributed in most parts of China as well as other tropical and subtropical countries or regions. The wide distribution of *C. argentea* supports its extensive applications. In this work, nine saponins and two phenylacetonitriles were isolated by column chromatography from *Semen Celosiae* and their structures were identified using mass spectrometry and NMR techniques (see ESI, Fig. S1–S39† for the data collected). In addition, two new compounds were obtained from *Semen Celosiae.*

In this work, many oleanane-type triterpenoid saponins were separated from *Semen Celosiae*, and such a process revealed that it contains high levels of oleanane-type triterpenoid saponins.[4] Due to the relatively large amounts of compounds **3**, **5**, **6**, **8**, and **9** obtained from *Semen Celosiae*, these compounds have potential to act as chemical markers for quality control of this plant, and so their contents in this plant were further determined. The results demonstrated that the seed part contained high concentrations of compounds **3**, **5**, and **6** which were all more than 0.8 mg g^{-1}. The content of compound **3** was almost twice as much as compounds **5**/**6**, and approximately ten times of compound **8**/**9** detected in the stir-fried and crude products, suggesting that compound **3** may be the key component for delegating the quality of *Semen Celosiae*.[23] Likewise, the contents of compounds **3**, **5**, **6**, **8**, and **9** remain well above the levels of compounds **2** and **10** which were a new class of chemical constituents found for the first time in *Semen Celosiae*. Accordingly, oleanane-type triterpenoid saponins are thought to be the major active com-

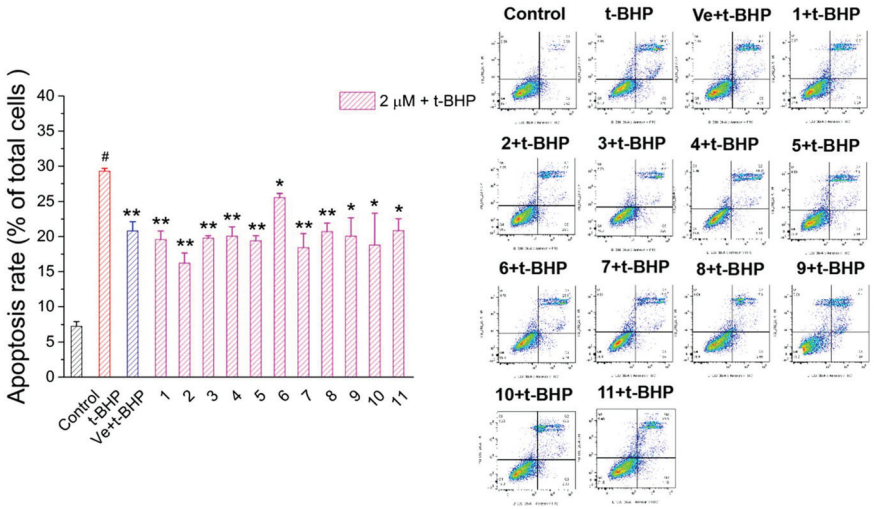

Fig. 9 Effect of compounds **1–11** on the apoptosis rate of motor neurons. #, $P < 0.01$ *versus* the control group; **, $P < 0.01$, *, $P < 0.05$ *versus* the *t*-BHP group.

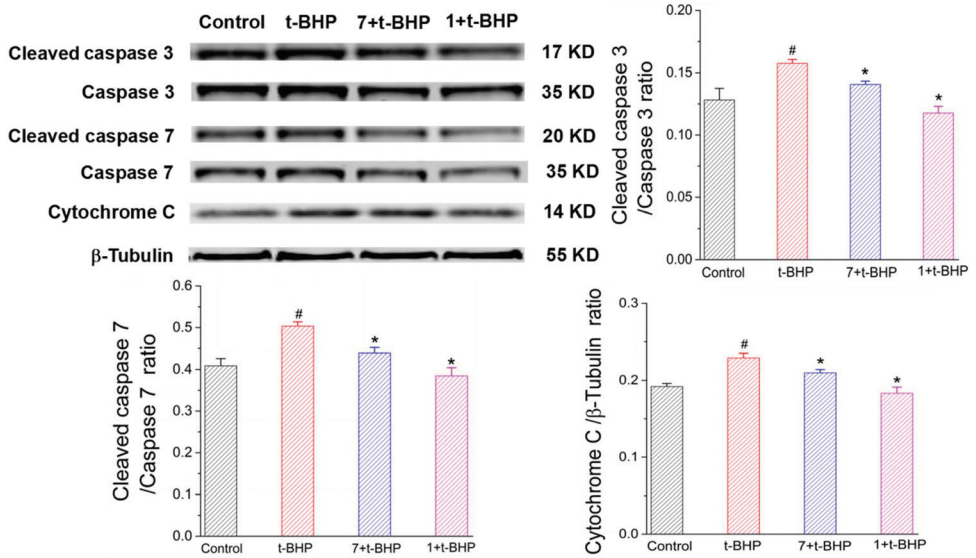

Fig. 10 The expression of caspase-3, cleaved caspase-3, caspase-7, cleaved caspase-7 and cytochrome C in neurons. β-Tubulin was used as a housekeeping protein. Data were presented as mean ± SD, $n = 3$ per group. # $P < 0.05$ *versus* the control group, * $P < 0.05$ *versus* the *t*-BHP group.

pounds of *Semen Celosiae.* In terms of concentrations of the five triterpenoid saponins and two phenylacetonitriles, there were some differences between the crude and stir-fried products. After stir-frying, the contents of compounds **2**, **3**, and **9** increased, while those of compounds **5**, **6**, and **8** decreased. However, the total concentration of the seven constituents (compounds **2**, **3**, **5**, **6**, and **8–10**) in the stir-fried product was much higher than that in the crude product, indicating that stir-frying may conduce to dissolving out the effective components from plant seeds.[24]

Notable health-promoting properties associated with saponins in *Semen Celosiae* include hepatoprotective effect, antitumor, antioxidative, and anti-inflammatory activities, *etc*. In contrast to the detailed accounts in other reports listing various activities after the intake of saponins,[4,8] the understanding of physiological effects of phenylacetonitrile glycosides remains limited. Given that the famous ancient document "Ben Cao Gang Mu" (the end of the 16th century) recorded the neuroprotective benefits of *Semen Celosiae*, there was a hypothesis that compounds **1–11** would possess such protective properties. To our knowledge, the present work is the first study which examines the neuroprotective effect of compounds **1–11** isolated from *Semen Celosiae* on cultured neurons.

It was reported that oxidative stress and free radical generation serve pivotal roles in neuronal loss and progression of

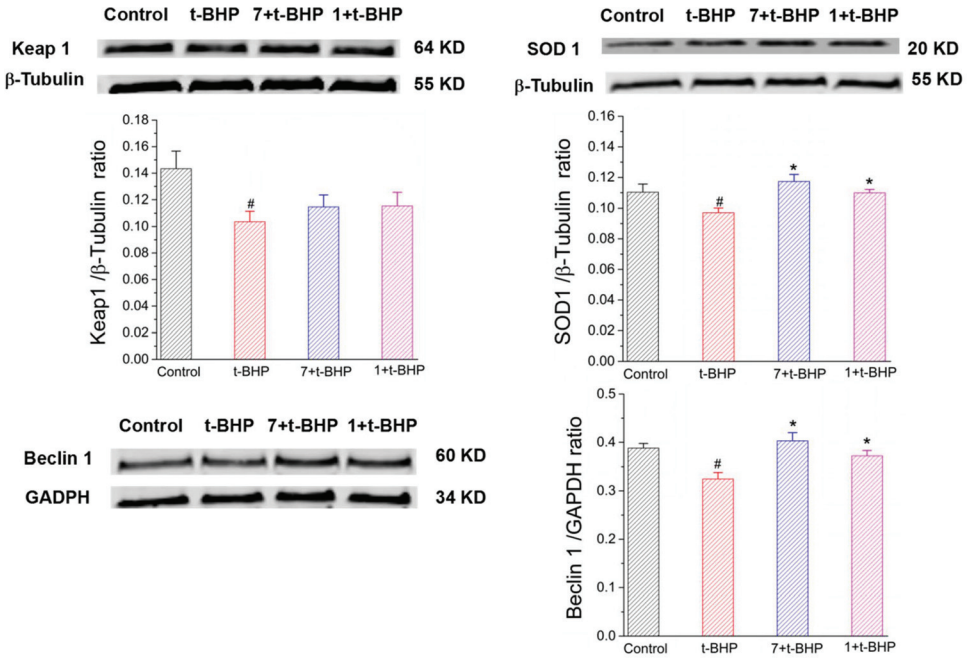

Fig. 11 The expression of Keap1, SOD1 and Beclin1 in neurons. β-Tubulin and GADPH were used as housekeeping proteins. Data are presented as mean ± SD, n = 3 per group. # $P < 0.05$ *versus* the control group, * $P < 0.05$ *versus* the *t*-BHP group.

neurodegenerative conditions.[25] NSC-34 cells were treated with *t*-BHP to induce oxidative injury. The protective effects of compounds **1–11** were investigated by CCK-8 assays (Fig. 6), and these results revealed that the viability of NSC-34 cells pretreated with compounds **1–11** was significantly much higher than that of the *t*-BHP group after exposure to *t*-BHP, indicating that compounds **1–11** might significantly enhance neuron survival and reduce oxidative damage.

Since *t*-BHP can easily penetrate cells and generate highly reactive hydroxyl radicals that successively attack cellular components including lipids, protein, and DNA, oxidative damage was thereby generated in cells. The mitochondrion is a major intracellular source of ROS and a target of high ROS exposure and has deleterious consequences.[9,26] The generation of ROS was quantified using the fluorescent probe CellROX red reagent. The red fluorescence indicates that the overproduction of ROS induces oxidative stress. It is observed that a decrease in *t*-BHP-induced ROS production in the NSC-34 cells pretreated with compounds **1–11** (Fig. 7) was further confirmed by confocal microscopy observation (Fig. 8). Increasing intracellular ROS formation causes apoptosis in neuronal cells. Apoptotic cell death is characterized by Annexin V-FITC/PI double staining. The results demonstrated that compounds **1–11** apparently reduced the apoptosis rate at a dosage of 2 μM, indicating that compounds **1–11** can effectively inhibit apoptosis induced by *t*-BHP.

Regarding the cell viability, ROS level, and apoptosis rate, compounds **1–11** all show different levels of activity. Compounds **1**, **6**, and **11** have the same aglycone structure, except for the relative configuration of substituents at the 2,3-position. Nevertheless, compound **1** exhibits an excellent protective effect compared with compounds **6** and **11**, suggesting that methylation of glucuronic acid in the 3-position, as well as α-orientations of substituents at the 2,3-position, may make a crucial contribution to compound **1**. Owing to the presence of glucose at the 28-position of compound **6**, its neuroprotective effect is evidently weak in contrast to compounds **1** and **11**, indicating that the glucose group at the 28-position may increase the hydrophilicity and steric hindrance[27] which prevent compound **6** from crossing the cell membranes to exert a protective effect on neural cells. Moreover, compounds **7–9** also have a similar structure, and one main difference among them is that different numbers of hydroxyl groups were observed at the A-ring part of compounds **7–9**. Among them, compound **7** displayed the lowest ROS level and apoptosis rate than the others. It can be concluded that the presence of these hydroxyl groups may trigger more effective neuroprotection. Interestingly, phenylacetonitriles are highly toxic, as the oral LD_{50} is 45.5 mg kg^{-1} for mice and 270 mg kg^{-1} for rats.[28] Similar to phenylacetonitrile glycosides with the same aglycone structure, compounds **2** and **4** did not show significant cytotoxicity in the range of 1–50 μM in NSC-34 cells. Compound **2** showed better protective capacity against *t*-BHP-induced cytotoxicity than compound **10**, indicating that different types of saccharide molecules linked at C-4 may affect their activities described in this work and diminish toxicity.[6]

In the present study, compounds **1–11** can protect from cell injury and improve the cell-survival rate, but the related mechanism remains obscure. Compounds **1** and **7** are two oleanane-type triterpenoid saponins, which are major active compounds of *Semen Celosiae*. Compound **1** is a new com-

pound and compound 7 shows an excellent protective capacity against *t*-BHP-induced cell apoptosis, so compounds **1** and **7** were chosen to investigate the mechanism of action.

When cells undergo apoptosis, some apoptosis-related proteins are activated or released.[29] Excessive activation of the apoptotic pathway eventually results in the neuronal loss in neurodegenerative diseases.[30,31] The following experimental results were in accordance with the observations above. Compounds **1** and **7** apparently decreased the ratio of cleaved caspase-3: caspase-3 and cleaved caspase-7: caspase-7 and the expression levels of cytochrome C to achieve an inhibitory effect on neuronal apoptosis. As mitochondria release more soluble proteins, cytochrome C for instance, they are involved in the mitochondria-mediated apoptotic pathway, which modulates the sensitivity to cell death signals to activate caspase cascade, and then cell apoptosis occurs.[32,33] The data discussed above suggested that compounds **1–11** effectively antagonized *t*-BHP-induced neuronal apoptosis.

Generally, beneficial antioxidative and antiapoptotic effects are closely associated with some anti-oxidant enzymes in many neurodegenerative disease therapies.[2] Superoxide dismutase (SOD), known as a detergent for free radicals in organisms, is the major enzyme responsible for the inactivation of superoxide and hydrogen peroxide. SOD1 is a major isoform of SOD, and is intimately involved in Parkinson's disease and amyotrophic lateral sclerosis, and also exerts a prominent role in the ROS-induced oxidative damage in neurodegeneration.[34] In the following study, it was found that compounds **1** and **7** up-regulated the protein expression of SOD1 in *t*-BHP-treated NSC-34 cells. In addition, they showed a significant effect on the expression of Keap1 protein compared with the *t*-BHP group. The Keap1–Nrf2 signaling pathway evokes an adaptive response to oxidative stress by regulating downstream antioxidant enzymes that serve to enhance cell survival.[35] Our computational molecular simulations demonstrated that compounds **1** and **7** failed to dock into the binding sites of Keap1 (PDB ID: 6QMC) (see ESI†), which was probably caused by their large dimensions and strong steric effect from surrounding residues.[36,37] Interestingly, the aglycone and sugar moiety of compounds **1** and **7** favorably docked to the active sites of Keap1 protein with a free binding energy ranging between −47.78 and −26.35 kcal mol^{-1} (see ESI†).

ROS also leads to the induction of autophagy at earlier time points which is a strong cell survival response and delays caspase activation. Autophagy plays a critical role in cell self-renewal, self-protection, tissue and organ development, growth, and differentiation.[38,39] The important autophagy-regulatory protein Beclin-1 can regulate autophagic cell death and apoptosis.[40] Dysregulated autophagy in neurocytes is related to the accumulation of oligomers and aggregates of misfolded proteins which is a characteristic of many neurodegenerative diseases. Autophagy upregulation can reduce the levels of toxic proteins, ameliorate signs of disease, and delay disease progression.[41] *t*-BHP-induced oxidative stress inhibited autophagy in the NSC 34 cells, which was significantly restored by compounds **1** and **7**. Moreover, compounds **1** and **7**-mediated autophagy may be instrumental in reversing *t*-BHP-induced oxidative stress and apoptosis. It is consistent with a previous report that the therapeutic effect of oleanane-type triterpenoid saponins extracted from *Semen Celosiae* on atherosclerosis may be related to the promotion of autophagy.[42] Wang *et al.* also indicated that autophagy was conducive to the neuroprotective effect of Eclalbasaponin I, an oleanane-type triterpenoid saponin.[7] The current research provides the first evidence that antioxidant and autophagic effects may be associated with the neuroprotective effect of compounds **1** and **7** from *Semen Celosiae* on *t*-BHP-induced motor neuron injury. In a word, the neuroprotective activities of compounds **1–11** from *Semen Celosiae* may provide some ideas for the development of therapeutic agents to treat neurodegenerative diseases.

5. Conclusion

The present work is the first systemic study to identify and evaluate the bioactive components extracted from the seeds of *Celosia argentea* L. for investigating their neuroprotective properties. Eventually, eleven constituents were successfully isolated from *Semen Celosiae* and their structures were further identified by the NMR data. Among them, two new compounds (**1** and **2**) were obtained, and four compounds (**4**, **7**, **9**, and **10**) were obtained from *Semen Celosiae* for the first time. The *in vitro* experiment firstly found that these compounds showed a significant protective effect against neuronal oxidative damage. The proposed mechanism may be involved in upregulating the antioxidative enzyme expression and activating the autophagy pathway. Therefore, *Semen Celosiae* may be regarded as a novel viable source of oleanane-type triterpenoid saponins and phenylacetonitrile glycosides with useful properties.

Conflicts of interest

The authors declare that there are no conflicts of interest.

Acknowledgements

The work was supported by 111 project of innovation and intelligence introduction base of crop's adversity biology (D16014), the Scientific and Technological Project of Henan Province (202102310519) and the National Science and Technology Major Project of the Ministry of Science and Technology of China (2018ZX09735005). We thank Sun Yat-sen University for providing computational resources. We also thank Dr Yuan Zhao at Henan University for helpful analysis in molecular docking.

References

1 M. T. Lin and M. F. Beal, Mitochondrial dysfunction and oxidative stress in neurodegenerative diseases, *Nature*, 2006, **443**, 787–795.

2 G. H. Kim, J. E. Kim, S. J. Rhie and S. Yoon, The Role of Oxidative Stress in Neurodegenerative Diseases, *Exp. Neurobiol.*, 2015, **24**, 325–340.
3 S. S. Bhujbal, S. S. Chitlange, A. A. Suralkar, D. B. Shinde and M. J. Patil, Anti- inflammatory activity of an isolated flavonoid fraction from Celosia argentea Linn, *J. Med. Plants Res.*, 2008, **2**, 52–54.
4 Y. Tang, H. L. Xin and M. L. Guo, Review on research of the phytochemistry and pharmacological activities of Celosia argentea, *Rev. Bras. Farmacogn.*, 2016, **26**, 787–796.
5 H. Qiu and X. Zeng, Nitrate, Nitrite and VC content from 6 species of wild vegetables produced in Guangdong, *Food Sci.*, 2004, **25**, 250–251.
6 X. Liu, Y. Sun, J. Bian, T. Han, D. Yue, D. Li and P. Gao, Neuroprotective effects of triterpenoid saponins from Medicago sativa L. against H_2O_2-induced oxidative stress in SH-SY5Y cells, *Bioorg. Chem.*, 2019, **83**, 468–476.
7 W. Wang, G.-D. Yao, X.-Y. Shang, J.-C. Gao, Y. Zhang and S.-J. Song, Eclalbasaponin I from Aralia elata (Miq.) Seem. reduces oxidative stress-induced neural cell death by autophagy activation, *Biomed. Pharmacother.*, 2018, **97**, 152–161.
8 Y. Zhang, W. Wang, H. He, X. Song, G. Yao and S. Song, Triterpene saponins with neuroprotective effects from a wild vegetable Aralia elata, *J. Funct. Foods*, 2018, **45**, 313–320.
9 C. Huang, C. Wen, M. Yang, D. Gan, C. Fan, A. Li, Q. Li, J. Zhao, L. Zhu and D. Lu, Lycopene protects against t-BHP-induced neuronal oxidative damage and apoptosis via activation of the PI3K/Akt pathway, *Mol. Biol. Rep.*, 2019, **46**, 3387–3397.
10 S. Y. Wang, C. Huang, R. K. Sun, L. N. Lu, H. G. Liang, L. Gao, J. Huang, J. H. Wang and B. F. Yang, New tirucallane triterpenoids from the dried latex of Euphorbia resinifera, *Phytochem. Lett.*, 2019, **29**, 220–224.
11 Henan Province Food and Drug Administration, *Processing norms of Chinese herbal medicine in Henan Province*, Henan Province people's Publishing House, Zhengzhou, 2005.
12 W. Nie, J. G. Luo and L. Y. Kong, New triterpenoid saponins from the roots of Gypsophila pacifica Kom, *Carbohydr. Res.*, 2010, **345**, 68–73.
13 P. K. Agrawal, NMR Spectroscopy in the structural elucidation of oligosaccharides and glycosides, *Phytochemistry*, 1992, **31**, 3307–3330.
14 S. Qiu, W. Z. Yang, C. L. Yao, X. J. Shi, J. Y. Li, Y. Lou, Y. N. Duan, W. Y. Wu and D. A. Guo, Malonylginsenosides with Potential Antidiabetic Activities from the Flower Buds of Panax ginseng, *J. Nat. Prod.*, 2017, **80**, 899–908.
15 Y. Jiang, F. J. Liu, Y. M. Wang and H. J. Li, Dereplication-guided isolation of novel hepatoprotective triterpenoid saponins from Celosiae Semen by high-performance liquid chromatography coupled with electrospray ionization tandem quadrupole–time-of-flight mass spectrometry, *J. Pharm. Biomed. Anal.*, 2017, **132**, 148–155.
16 H. Zhang, Z. X. Liao and J. M. Yue, Cyano- and nitro-containing compounds from the roots of Semiaquilegia adoxoides, *Chin. J. Chem.*, 2010, **22**, 1200–1203.
17 Y. Koike, M. Fukumura, Y. Hirai, Y. Hori, S. Usui, T. Atsumi and K. Toriizuka, Novel phenolic glycosides, adenophorasides A–E, from Adenophora roots, *J. Nat. Med.*, 2010, **64**, 245–251.
18 X. Pang, H. X. Yan, Z. F. Wang, M. X. Fan, Y. Zhao, X. T. Fu, C. Q. Xiong, J. Zhang, B. P. Ma and H. Z. Guo, New oleanane-type triterpenoid saponins isolated from the seeds of Celosia argentea, *J. Asian Nat. Prod. Res.*, 2014, **16**, 240–247.
19 S. Wei, H. Liang, Y. Zhao and R. Zhang, Separation and identification of the compounds from Achyranthes bidentata BL, *China J. Chin. Mater. Med.*, 1997, **22**, 293–295.
20 X. Liu, J. Zhang, K. Guo, A. Jia, M. Zhang, Y. Shi, C. Liu, L. Xiao and Z. Sun, Three new oleanane-type triterpenoid saponins from the seeds of Celosia cristata L, *Nat. Prod. Res.*, 2018, **32**, 167–174.
21 H. Wei, Y. Li, J. Chen and P. Li, Triterpenoid saponins from Achyranthes bidentata, *Chin. J. Nat. Med.*, 2012, **10**, 98–101.
22 Q. Xue, Z. L. Sun, M. L. Guo, Y. Wang, G. Zhang and X. K. Wang, Two new compounds from Semen celosiae and their protective effects against CCl 4 -induced hepatotoxicity, *Nat. Prod. Res.*, 2011, **25**, 772–780.
23 Y. Wang, Y. Yu and H. Li, Assay of celosin I in Celosiae Semen by HPLC-ELSD, *Chin. Tradit. Pat. Med.*, 2013, **35**, 1957–1961.
24 Compilation Committee of Processing Chinese Material Science Medica, *Science of processing Chinese materia medica*, People's Medical Publishing House, Beijing, 2nd edn, 2015.
25 Y. Christen, Oxidative stress and Alzheimer disease, *Am. J. Clin. Nutr.*, 2000, **71**, 621S–629S.
26 J. C. Martinou and R. J. Youle, Mitochondria in Apoptosis: Bcl-2 Family Members and Mitochondrial Dynamics, *Dev. Cell*, 2011, **21**, 92–101.
27 X. L. Meng, J. Y. Yang, G. L. Chen, L. H. Wang, L. J. Zhang, S. Wang, J. Li and C. F. Wu, Effects of resveratrol and its derivatives on lipopolysaccharide-induced microglial activation and their structure–activity relationships, *Chem.-Biol. Interact.*, 2008, **174**, 51–59.
28 X. Ma, J. Deng, J. Feng, N. Shanaiah, E. Smiley and A. M. Dietrich, Identification and characterization of phenylacetonitrile as a nitrogenous disinfection byproduct derived from chlorination of phenylalanine in drinking water, *Water Res.*, 2016, **102**, 202–210.
29 Z. Zare, S. Zarbakhsh, M. Tehrani and M. Mohammadi, Paraoxon-induced damage in rat hippocampus is associated with alterations in the expression of apoptosis-related proteins, *Pestic. Biochem. Physiol.*, 2020, **166**, 104580–104588.
30 K. Sadek, T. Abouzed and S. Nasr, Lycopene modulates cholinergic dysfunction, Bcl-2/Bax balance, and antioxidant enzymes gene transcripts in monosodium glutamate (E621) induced neurotoxicity in a rat model, *Can. J. Physiol. Pharmacol.*, 2016, **94**, 394–401.
31 W. Z. Li, W. P. Li, W. Zhang, Y. Y. Yin, X. X. Sun, S. S. Zhou, X. Q. Xu and C. R. Tao, Protective Effect of Extract of Astragalus on Learning and Memory Impairments and

Neurons Apoptosis Induced by Glucocorticoids in 12-Month Male Mice, *Anat. Rec. Adv. Integr. Anat. Evol. Biol.*, 2011, **294**, 1003–1014.

32 M. Wines-Samuelson, E. C. Schulte, M. J. Smith, C. Aoki, X. Liu, R. J. Kelleher and J. Shen, Characterization of Age-Dependent and Progressive Cortical Neuronal Degeneration in Presenilin Conditional Mutant Mice, *PLoS One*, 2010, **5**, e10195.

33 R. A. Fuentealba, Q. Liu, T. Kanekiyo, J. Zhang and G. Bu, Density Lipoprotein Receptor-related Protein 1 Promotes Anti-apoptotic Signaling in Neurons by Activating Akt Survival Pathway, *J. Biol. Chem.*, 2009, **284**, 34045–34053.

34 P. Milani, G. Ambrosi, O. Gammoh, F. Blandini and C. Cereda, SOD1 and DJ-1 Converge at Nrf2 Pathway: A Clue for Antioxidant Therapeutic Potential in Neurodegeneration, *Oxid. Med. Cell. Longevity*, 2013, **2013**, 1–12.

35 B. Cui, S. Zhang, Y. Wang and Y. Guo, Farrerol attenuates β-amyloid-induced oxidative stress and inflammation through Nrf2/Keap1 pathway in a microglia cell line, *Biomed. Pharmacother.*, 2019, **109**, 112–119.

36 Y. Zhao, N. Chen, C. Wang and Z. Cao, A Comprehensive Understanding of Enzymatic Catalysis by Hydroxynitrile Lyases with S Stereoselectivity from the α/β-Hydrolase Superfamily: Revised Role of the Active-Site Lysine and Kinetic Behavior of Substrate Delivery and Sequential Product Release, *ACS Catal.*, 2016, **6**, 2145–2157.

37 Y. Zhao, N. She, Y. Ma, C. Wang and Z. Cao, A Description of Enzymatic Catalysis in N -Acetylhexosamine 1-Kinase: Concerted Mechanism of Two-Magnesium-Ion-Assisted GlcNAc Phosphorylation, Flexibility Behavior of Lid Motif upon Substrate Recognition, and Water-Assisted GlcNAc-1-P Release, *ACS Catal.*, 2018, **8**, 4143–4159.

38 P. Wang, C. Huang, J. Gao, Y. Shi, H. Li, H. Yan, S. Yan and Z. Zhang, Resveratrol induces SIRT1- Dependent autophagy to prevent H_2O_2-Induced oxidative stress and apoptosis in HTR8/SVneo cells, *Placenta*, 2020, **91**, 11–18.

39 M. Ishaq, M. A. Khan, K. Sharma, G. Sharma, R. K. Dutta and S. Majumdar, Gambogic acid induced oxidative stress dependent caspase activation regulates both apoptosis and autophagy by targeting various key molecules (NF-κB, Beclin-1, p62 and NBR1) in human bladder cancer cells, *Biochim. Biophys. Acta, Gen. Subj.*, 2014, **1840**, 3374–3384.

40 Q. Sun, W. Gao, P. Loughran, R. Shapiro, J. Fan, T. R. Billiar and M. J. Scott, Caspase 1 Activation Is Protective against Hepatocyte Cell Death by Up-regulating Beclin 1 Protein and Mitochondrial Autophagy in the Setting of Redox Stress, *J. Biol. Chem.*, 2013, **288**, 15947–15958.

41 A. Djajadikerta, S. Keshri, M. Pavel, R. Prestil, L. Ryan and D. C. Rubinsztein, Autophagy Induction as a Therapeutic Strategy for Neurodegenerative Diseases, *J. Mol. Biol.*, 2020, **432**, 2799–2821.

42 Y. Tang, H. Wu, B. Z. Shao, Y. Q. Wang, C. Liu and M. L. Guo, Celosins inhibit atherosclerosis in ApoE-/- mice and promote autophagy flow, *J. Ethnopharmacol.*, 2018, **215**, 74–82.

